Static Stability Analysis of Hexagonal Hexapod Robot for the Periodic Gaits

Article · September 2014

CITATIONS
2

READS
117

2 authors:

Firas Abdulrazzaq Raheem
University of Technology, Iraq
19 PUBLICATIONS **8** CITATIONS
SEE PROFILE

Hind Z. Khaleel
University of Technology, Iraq
5 PUBLICATIONS **3** CITATIONS
SEE PROFILE

Static Stability Analysis of Hexagonal Hexapod Robot for the Periodic Gaits†

Dr. Firas A. Raheem[1], Hind Z. Khaleel[2]

[1]Control and Systems Engineering Department, University of Technology, Baghdad-Iraq

[2]Control and Systems Engineering Department, University of Technology, Baghdad-Iraq

e-mail: dr.firas7010@yahoo.com, hhindzuhair@yahoo.com

Received: 26/05/2014

Accepted: 11/09/2014

Abstract – Hexagonal hexapod robot is a flexible mechanical robot with six legs. It has the ability to walk over terrain. The hexapod robot likes insect so it has the same periodic gaits. These gaits are tripod, wave and ripple gaits. Hexapod robot needs to stay statically stable at all the times during each gait in order not to fall with three or more legs continuously contacts with the ground. The safety static stability walking can be indicated by the stability margin. In this paper we based on the forward, inverse kinematics for each hexapod's leg to simulate the hexapod robot model walking for all periodic gaits and the geometry in order to derive the equations of the sub-constraint workspaces for each hexapod's leg. They are defined as the sub-constraint workspaces volumes when the legs are moving without collision with each other and they are useful to keep the legs stable from falling during each gait. A smooth gait was analyzed and enhanced for each hexapod's leg in two phases, stance phase and swing phase. The equations of the stability margins are derived and computed for each gait. The simulation results of our enhanced path planning of the hexapod robot approach whish's include all the gaits are statically stable and we are compared between all stability margins for each gait. In addition, our results show clearly that the tripod gait is the fastest gait while the wave and the ripple gaits are more stable than the tripod gait but the last one has less peaks of stability margins than others.

Keywords – Kinematics, Stability margin, Workspace, Hexapod robot.

† *This paper has been presented in ECCCM-2 Conference* and accredited for publication according to IJCCCE rules.

1. Introduction

Multi-legged robots display significant advantages with respect to wheeled ones for walking over rough terrain because they do not need continuous contact with the ground. In Multi-legged robots, hexapod robots, mechanical vehicles that walk on six legs, have attracted considerable attention in recent decades. There are several benefits for hexapods rover such as: efficient one to maintain for statically stable static on three or more legs, it has a great deal of flexibility in how it can move [1]. Legs do less damage to the ground than tracks and wheels [2]. During the walking of the legged robot, there is a difficult problem of generation and control of the sequence of placing and lifting of legs such that at any instant body should be stable and capable of moving from one position to other. The generation and sequence of such leg motion is called gait [3].Hexapod robot looks like insect so it has the same gait. If a similar state of the same leg during successive strokes in the same time for all legs called "periodic gait" [1].These gaits are: Wave gait, Ripple gait, and Tripod gait [4]. The optimally stable range of the wave gait has been studied in [5]. While [6] calculated the loss stability for the phase modification of the wave gaits. In [7] presented a new criterion for the asymptotic stance stability of a statically balanced legged robot.

In this paper the main problem is when hexapod robot walking and may be fall down if the legs are not constraints so the static stability is analyzed according to constraints of each leg in order not to fall.

2. Modeling of Hexapod Robot

The legged locomotion verities by verity of usual terrain and it presents a set of difficult problems (foot placement, obstacle avoidance, load distribution, common stability) which must be taken into account both in mechanical construction of vehicles and in development of control strategies [8]. Besides that, these issues are using models that mathematically explain the verities of situations and for that; the robot modeling becomes a practical tool in understanding systems complexity and for testing and simulating diverse control approaches [9].The robot structure considered has (6) identical legs and each leg has (3) degree of freedom, in addition to that, all the related points for each joint have been put on the model, the legs numbering as shown in Fig. 1, robot's center coordinate o (x_o, y_o, z_o).

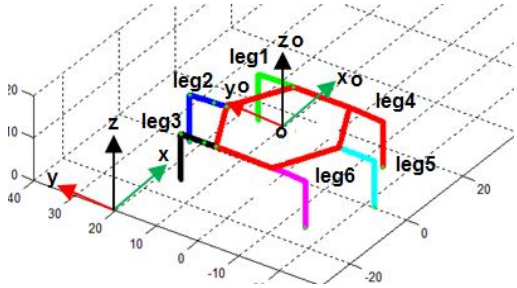

Figure 1.Hexapod robot structure

The z-axis pointing up, the x-axis pointing forward and the y-axis pointing left. Hexapod modeling consisting of two types, one is forward kinematic and its inverse, below will discuss in details for each type of kinematic.

2.1. Forward kinematics for One Leg of hexapod robot

The successful design of a legged robot depends to a large amount on the leg design chosen. Since all aspects of walking are ultimately governed by the physical limitations of the leg, it is important to select a leg that will allow a maximum range of motion and that will not inflict unnecessary constraints on the walking [10]. A three-revolute kinematical chain (R_1, R_2, R_3) has been

chosen for each leg mechanism in order to imitate the leg structure as shown in Fig. 2. A direct geometrical model for each leg mechanism is formulated between the moving frame $o_i(x_i, y_i, z_i)$ of the leg base, where i=1…6, and the fixed frame o (x_o, y_o, z_o) [10].

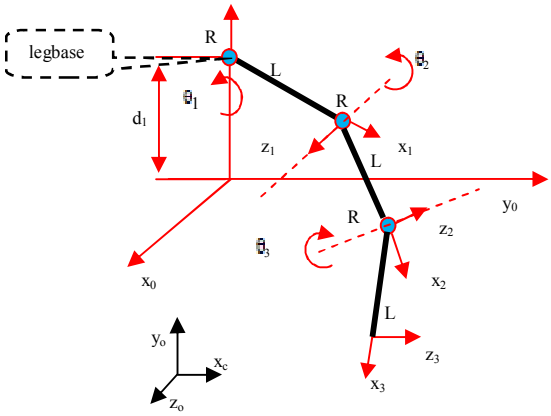

Figure 2. Model and coordinates frame for leg kinematics.

In this paper the BH3-R hexapod robot is taken as a case study of hexagonal hexapod robot. The lengths of the hexapod's leg are: L_1 = (2.9 cm), L_2 = (5.7 cm), L_3 = (10.8 cm) [11]. The robot leg frame starts with link (0) which is the point on the robot body where the leg is jointed to; link (1) is the coxa, link (2) is the femur and link (3) is the tibia. Legs are distributed symmetrically around the axis in the direction of motion (x in this case). The general form for the transformation matrix from link (i) to link $(i\text{-}_1)$ using Denavit Hartenberg parameters are given in (1) [10, 12]:

$$T_i^{i-1} = \begin{bmatrix} \cos\theta_i & -\sin\theta_i\cos\alpha_i & \sin\theta_i\sin\alpha_i & a_i\cos\theta_i \\ \sin\theta_i & \cos\theta_i\cos\alpha_i & -\cos\theta_i\sin\alpha_i & a_i\sin\theta_i \\ 0 & \sin\alpha_i & \cos\alpha_i & d_i \\ 0 & 0 & 0 & 1 \end{bmatrix} \quad (1)$$

The transformation matrix is a series of transformations:

1. Translate d_i along z_{i-1} axis.
2. Rotate $\theta_i$about z_{i-1} axis.
3. Translate α_i about x_{i-1} axis.
4. Rotate α_i about x_{i-1} axis.

The overall transformation is obtained as a product between three transformation matrixes:

$$T_{coxa}^{base} = T_{coxa}^{femur} T_{femur}^{tibia} \quad (2)$$

Considering Fig. 2 and using (2) the coordinates of the leg tip are:

$$\begin{aligned} x &= \cos\theta_1 * (L_1 + L_2 * \cos\theta_2 + L_3 * \cos(\theta_2 - \theta_3)), \\ y &= \sin\theta_1 * (L_1 + L_2 * \cos\theta_2 + L_3 * \cos(\theta_2 - \theta_3)), \\ z &= d_1 + L_2 * \sin\theta_2 + L_3 * \sin(\theta_2 - \theta_3). \end{aligned} \quad (3)$$

Where: d_1 is the distance from the ground to the coxa joint. L_i are the lengths of the leg links.

2.2. Inverse kinematics

The geometrical model described above establishes a link between the joint variable and the position and orientation of the end frame. The inverse kinematics problem consists of formative the joint angles from a given position and orientation of the end frame. The solution of this problem is significant in order to transform the motion assigned to the end frame into the joint angle motions matching to the desired end frame motion. The goal is to find the three joint variables θ_1, θ_2, and θ_3 corresponding to the desired end frame position. The end frames orientation is not a matter, since only paying attention in its position [10].

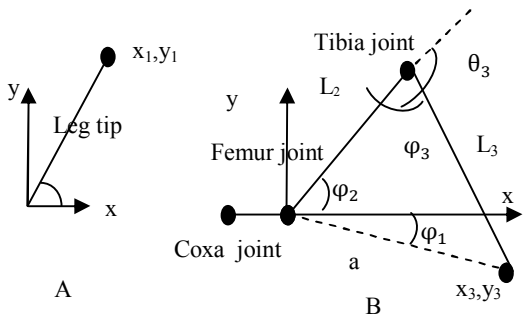

Figure 3 Illustrations for solving inverse kinematics.

Using (3) and considering the following constraints: all joints allow rotation only about one axis, femur and tibia always rotate on parallel axes, and the physical limitation of each joint represents the joint angle.

The coxa joint angle can be found using atan2(y,x) function as can be seen from Fig. 3 A.

$$\theta_1 = \operatorname{atan2}(y_1, x_1) \tag{4}$$

In order to determine the other two angles a geometrical approach was considered. To further simplify the approach the leg tip coordinates were transformed to coxa frame using the transformation matrix below:

$$T_{coxa}^{femur} = \begin{pmatrix} (R_{femur}^{coxa}) & -(R_{femur}^{coxa})^T * d_{femur}^{coxa} \\ 0 & 1 \end{pmatrix} \tag{5}$$

An angle φ_2 which is the angle relating to the femur servo position, can be derived directly from the triangle Fig. 3 B.

$$\theta_2 = \varphi_2 \tag{6}$$

The angle φ_1 is the angle between the x-axis and line a, and can be calculated with atan2 function:

$$\varphi_1 = \operatorname{atan2}(y_3, x_3) \tag{7}$$

Where x3 and y3 are the leg tip coordinates in coxa frame. If it considers φ_t being the entire femur span and apply the law of cosines results:

$$\varphi_t = \operatorname{acos}\left(\frac{L_2^2 + a^2 - L_3^2}{2 * L_2 * a}\right) \tag{8}$$

Where:

$$a = \sqrt{x_3^2 + y_3^2} \tag{9}$$

Next the femur angle can be found from:

$$\theta_2 = \operatorname{acos}\left(\frac{L_2^2}{2\,L_2 * L_3}\right) + \operatorname{atan2}(y_3, x_3) \tag{10}$$

Again, applying the law of cosines to find the φ_3 angle:

$$\varphi_3 = \operatorname{acos}\left(\frac{L_2^2 + L_3^2 - a^2}{2\,L_2 * L_3}\right) \tag{11}$$

Considering Fig. 3 B, the θ_3 can be found as follows [10]:

$$\theta_3 = \pi - \varphi_3 \tag{12}$$

3. The Stability Analysis and Constraint Workspace

In this paper, the two methods of one leg workspace are analyzed:

3.1. Workspace of Hexapod's Leg

In this paper the Hexapod's leg workspace has been computed and analyzed. Hexapod's leg workspace can defined as the set of reachable points by the end-effector for each foot. These points (positions) depended on the leg orientation (the mechanical limits of the joints). The mechanical limits of the joints restrict leg motion and are a major factor to consider when developing walking algorithm for a hexapod module. The working volumes for each leg are identical because each leg of hexapod has the same geometrical configuration and joint limits; the analyation of the two approaches is evaluated the constraint workspace for BH3-R hexapod robot [11]. The limits of the joint variables for a representative one leg are shown in Table1.

Table 1. Range of angles for one hexapod's leg.

Link Name	The range of one robot's leg angle in degree
Coxa	$-90 < \theta_1 < 90$
Femur	$-45 < \theta_2 < 90$
Tibia	$0 < \theta_3 < 135$

These joint variable limits, then, separate the reachable area from the unreachable area. Reachable areas move with the body. The region included within the reachable area is known as the unconstrained working volume (UWV).

The constrained working volume (CWV) is defined as a subset of the original working volume, for each leg, that ensures static stability.

Therefore, the (CWV) sets soft limits for each leg so as to exclude points from the working volume that may lead to instability. In our case, the working volume is also constrained to prevent leg collisions. An excluded area for hexapod's legs, then, is that part of the reachable area where, if a foot were placed there, instability or leg collision might result.

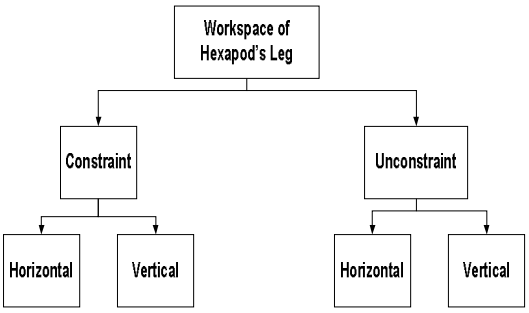

Figure 4.Flowchart Workspace of hexapod's leg

Figure 4 shows that the flowchart of workspace. The workspace of robot leg is computed from kinematics and geometry as follow:

3.1.1. Unconstrained Workspace

The unconstrained horizontal workspace of hexapod leg is the reachable areas include the sections in the xy plane around the individual coxas and within the mechanical joint limits, the y plane equal (33.15 cm). The unconstrained vertical workspace, or z-plane reachable area, depends on the height of the hexapod's center-of-body above the terrain is (5.5 cm). To define the maximum unconstrained vertical workspace, If a leg were extended to its fullest, the added lengths of radius body (13.75 cm), coxa (2.9 cm), femur (5.7 cm), and tibia (10.8 cm) y-plane would equal (33.15 cm). The minimum unconstrained vertical workspace, If a leg were lack extent to its fullest, ($\theta_3 = 135^0$) the y-plane would equal (14.7cm) while the z-plane equal (9 cm).

3.1.2. Constrained Workspace

The CWV used in this paper results from six basic constraints:

- the height (z = plane) from the ground to the CB (center body of robot) = (10.8 cm) is fixed for minimum, maximum reach, the vertical maximum reach equal (24.25 cm) if $\theta_3 = 80^0$ and minimum reach equal (21 cm) if $\theta_3 = 97^o$,
- the suitable posture of robot = (22.35 cm) if $\theta_3 = 90^o$,
- The terrain is flat,
- The legs are not allowed to collide or overlap, and
- The horizontal workspace of hexapod leg is The reachable areas include the sections in the xy plane around the individual coxas, y-plane = 24.25 cm and within the mechanical joint limits but in this case limit joint (in proposed method, the half range of coxa angle is taken in order not to the legs collide) soothe range is $(-45 < \theta_1 < 45)$ degree. Another approach is derived for Constrained Workspace more details in [13], [14]. For the hexagonal model the mathematically (13) for the radius of the annulus is :

$$r_{max}^2 = (r_{min} + Q)^2 + \left(\frac{1}{2} * P\right)^2 \quad (13)$$

Where: r_{max}, r_{min}, Q, P defined by Fig. 5.

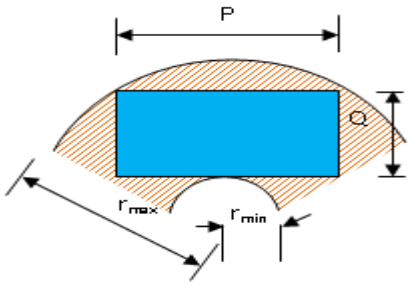

Figure 5.The relationship between the reachable area and annuls.

The rectangular area is the reachable area of each leg of robot, for our hexapod robot r_{max} = (10.5cm) from coxa joint. Added the length of center robot (13.75 cm), r_{max} = (24.25 cm). The center of leg tip point is (22.35 cm) that it is equal to the posture robot in method1 above comparing between two constraints workspaces methods and found that the maximum reaches of the leg are equal for our hexapod robot.

3.2. Static Stability analysis of hexapod robot

The first gait of the hexapod robot is the tripod gait. In this gait the three legs stay on the ground (support pattern) while the other legs are on the air. The analysis of static stability depended on the (14) in [15] that only compute the S_1, S_2 and S_3 in the Fig. 6 of three triangles and there are two conditions to set the robot stable first If S_1, S_2 and $S_3$are >= zero, the tripod is considered stable other, the tripod is considered unstable more details in [15].
From the definition of "stability margin," (sm),is the shortest distance from the vertical projection of the center of robot to the boundaries of the support pattern in the horizontal plane [5] the proposed method explained as below:
In Fig. 6 derived L1 is derived in (16) (the distance line between two points) and the same thing for L_2, L_3 are computed for other legs, each L is considered as a base of the one triangle while the areas of the S_1, S_2 and S_3 are previously computed so that the stability margin is the shortest perpendicular distances from L_1, L_2 and L_3 to the center of robot (H_1, H_2, H_3 respectively). H_1 is computed as in (17) as well as the H_2, H_3 are computed in the same manner. The stability margins are analyzed and computed for all cases of the legs motion for three gaits (tripod, ripple, wave) of hexapod robot as below:

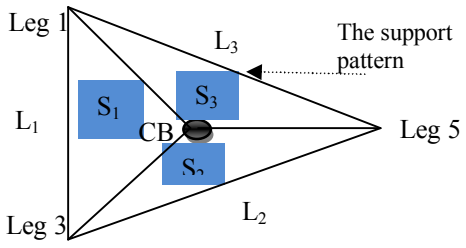

Figure 6.The stability analysis for the tripod gait when legs (1, 3, 5) on the ground.

The triple equation of the Fig. 6 is:

$$S_1 = \frac{1}{2}\begin{vmatrix} 1 & 1 & 1 \\ x_{CB} & x_1 & x_3 \\ y_{CB} & y_1 & y_3 \end{vmatrix} \quad (14)$$

Where (x_{CB}, y_{CB}) is the coordinate of CB point, (x_1, y_1) the coordinate of Leg 1, (x_3, y_3) the coordinate of Leg3.
With expansion:

$$S_1 = \frac{1}{2}[(x_1 - x_{CB})(y_3 - y_{CB}) - (x_3 - x_{CB})(y_1 - y_{CB})] \quad (15)$$

$$L_1 = \text{sqrt}((x_3 - x_1)^2 + (y_3 - y_1)^2) \quad (16)$$

Where L_1 is the distance between two points

$$H_1 = 2 * \left(\frac{S_1}{L_1}\right) \quad (17)$$

From other triangles as shown in Fig. 6 the stability margin is computed as:

$$sm_1 = \min(H_1, H_2, H_3) \quad (18)$$

$sm_1$is the stability margin of the support pattern of legs (1,3,5), similarly, $sm_2$is derived for other three legs (2,4,6) as shown in Fig. 7 where the legs (2,4,6) are stance on the ground and (1,3,5) in the air. Also, (18) is derived for the other gaits of robot (wave and ripple).

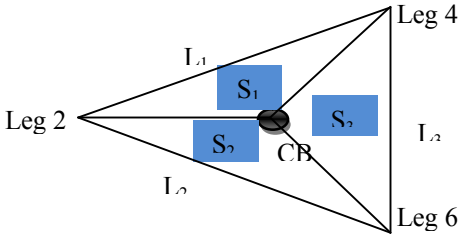

Figure 7.The stability analysis for the tripod gait when legs (2,4,6) on the ground.

In the wave gait only one leg in the air, while the others are on the ground so the support pattern is divided into five areas (S_1, S_2, S_3, S_4, S_5) and the stability margin is evaluated for all the cases of wave gait as shown below:

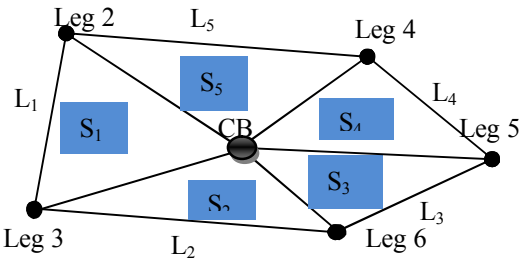

Figure 8. Case 1 representation where the support pattern (legs (2,3,4,5,6) on ground) of the wave gait.

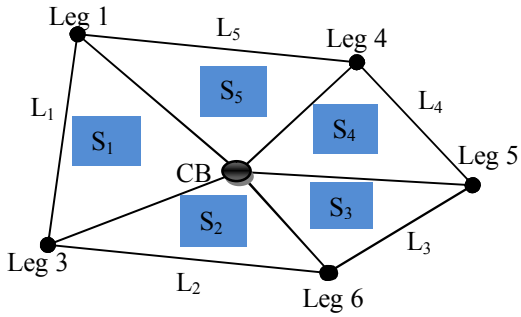

Figure 9. Case 2 representation where the support pattern (legs (1,3,6,5,4) on ground) of the wave gait.

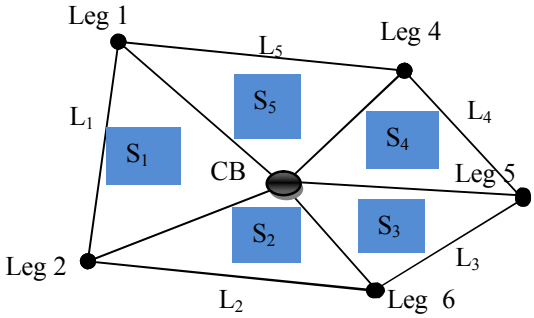

Figure 10. Case 3 representation where the support pattern (legs (1,2,6,5,4) on ground) of the wave gait.

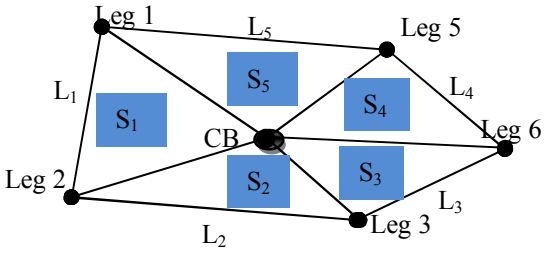

Figure 11. Case 4 representation where the support pattern (legs(1,2,3,6,5) on ground) of the wave gait.

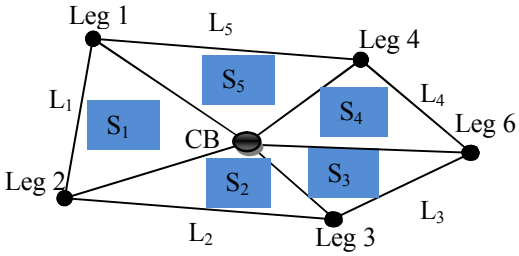

Figure 12. Case5 representation where the support pattern (legs(1,2,3,6,4) on ground) of the wave gait.

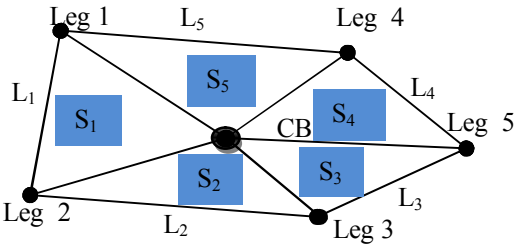

Figure 13. Case 6 representation where the support pattern (legs(1,2,3,5,4) on ground) of the wave gait.

The stability margins of the ripple gaits as shown:

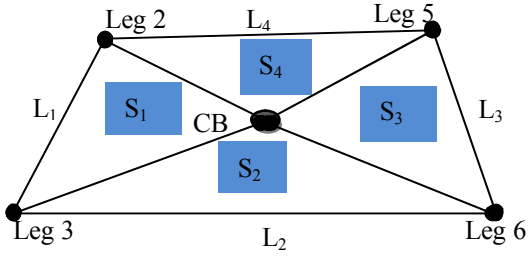

Figure 14. Case 1 representation where the support pattern (legs (2,3,6,5) on ground) of the ripple gait.

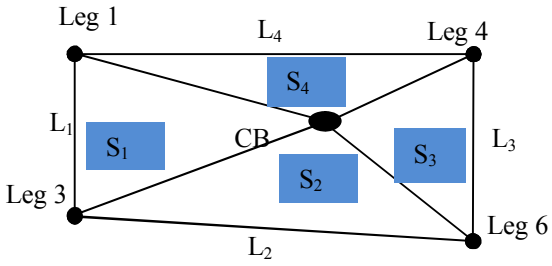

Figure 15. Case 3 representation where the support pattern (legs (1,3,6,4) on ground) of the ripple gait.

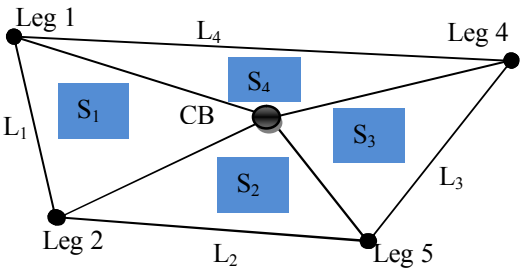

Figure 16. Case 4 representation where the support pattern (legs (1,2,5,4) on ground) of the ripple gait.

4. Walking and path planning of hexapod robot:

The path planning and algorithm of legs walking are explained as below:

4.1. The mechanism of leg motion:

The mechanism of leg motion is very complex problem that each leg is forward and back motion. It derived from insect motion that has two phases: swing (the leg in the air) and stance (the leg in the ground) phases [4].Equations of motion in [16] are derived for two phases. The walking of hexapod robot is developed by combing the stance phase [16] explained by (19) and the swing phase [17] as in (20) to get our modified smooth gait for one hexapod's leg as below:

$$xtip_{i+1} = xtip_i + \frac{v*\cos(\phi)}{2},$$
$$ytip_{i+1} = ytip_i + \frac{v*\sin(\phi)}{2}. \quad (19)$$

Where $xtip_i, ytip_i$the coordinates of leg tip derived from the forward kinematic, ϕ is the direction of motion and v describes how many centimeters per gait cycle the hexapod robot should move.
The equations in swing phase are:

$$x_{tip_i} = 2 * \dot{x} * dt(1 - \cos\left(\frac{\pi t}{dt}\right)),$$
$$y_{tip_i} = 2 * \dot{y} * dt(1 - \cos\left(\frac{\pi t}{dt}\right)),$$
$$z_{tip_i} = h * (1 - \cos\left(\frac{\pi t}{dt}\right)). \quad (20)$$

$\dot{x}$, $\dot{y}$ are the speed of the hexapod robot's truck in x and y directions,dt is the time duration for each step and h is the height of each step. After explained the mechanism of leg motion, there is a need to show the movement of the center of body that moves from start point to the goal point so the new center point [15] is calculated as:

$$CB_{x_{i+1}} = CB_{x_i} + L * \cos(\phi),$$
$$CB_{y_{i+1}} = CB_{y_i} + L * \sin(\phi). \quad (21)$$

Where L is the step size.
The start point (0,0) and goal point (100,0) for the straight line.

5. Simulation Results

The analysis of the stability margins above for three gaits (ripple, wave, and tripod) are discussed and simulated for each gait within the steps as below:

a- The ripple gait cases

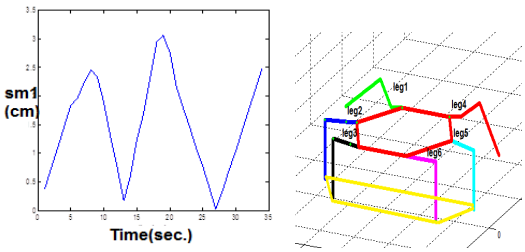

Figure 17. The final sm_1= 2.4724 cm while the robot lift two forward legs (1,4).

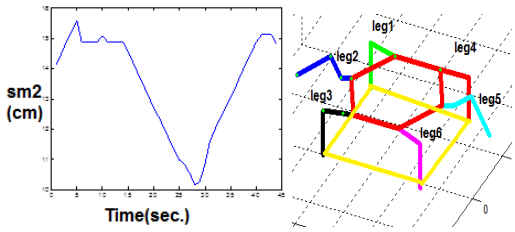

Figure 18. The final sm_2= 14.7998 cm when the robot lift middle legs (2,5).

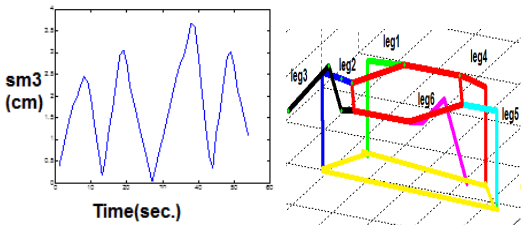

Figure 19. The last case of ripple gait in when the robot lift middle legs (3,6) so the final value of sm_3= 1.0666.

The sm_2 is more stable and larger support pattern than sm_1 and sm_2 the last stabilities values near to zero (critical stable).

b- The wave gait cases

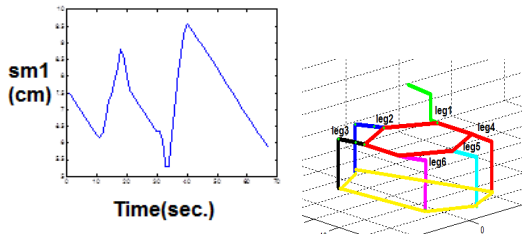

Figure 20. The wave gait the sm_1=6.0045 cm for lifting leg 1.

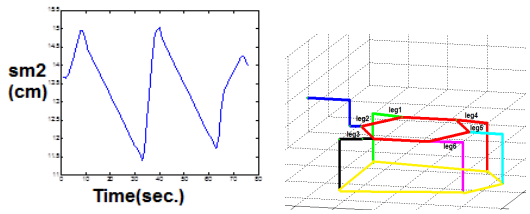

Figure 21. The robot lift middle left leg 2, the sm_2 = 13.9733 cm.

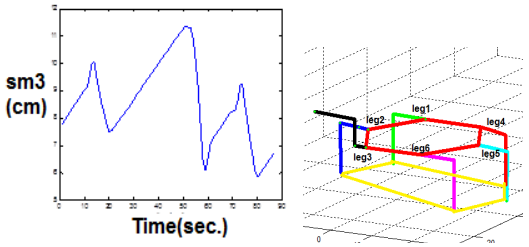

Figure 22. The robot lifting leg 3 the sm_3= 6.6249 cm.

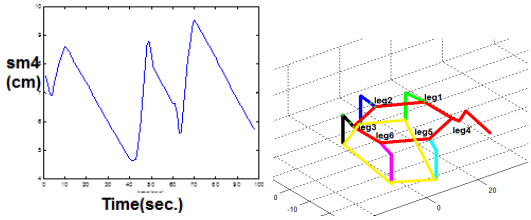

Figure 23. The hexapod robot lift forward leg 4 so the sm_4= 5.9669 cm.

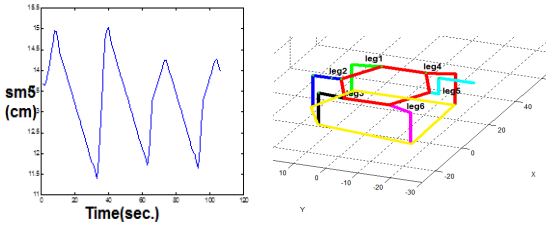

Figure 24. The robot lift the middle leg 5 and the sm_5= 13.9808 cm.

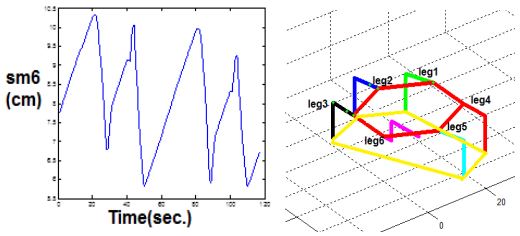

Figure 25. The last case of the robot lift the last leg 6 while the sm_6= 6.5843cm.

The results of sm for two figures (21-24) show that most stable values with the other wave gait cases.

c- Tripod gait cases

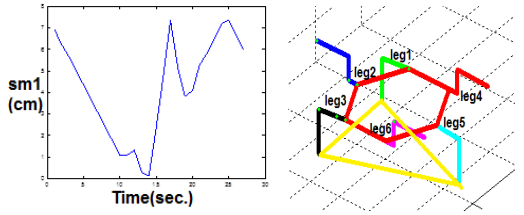

Figure 26. The sm_1= 6.6804 cm when the robot lifting three even legs (2,4,6).

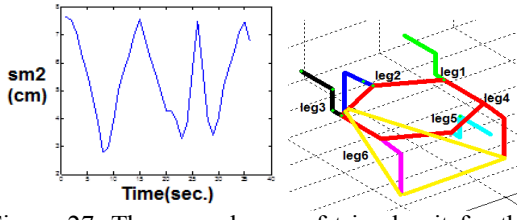

Figure 27. The second case of tripod gait for the sm_2= 6.7628 cm when the robot lifting three odd legs (1,3,5).

The two results of stability margins and the support pattern (i.e the yellow lines of legs on the ground in the simulation) are nearly equal for tripod gait.

From the development path planning for hexapod walking, the one case from above all cases is compared as shown in Fig. 28.

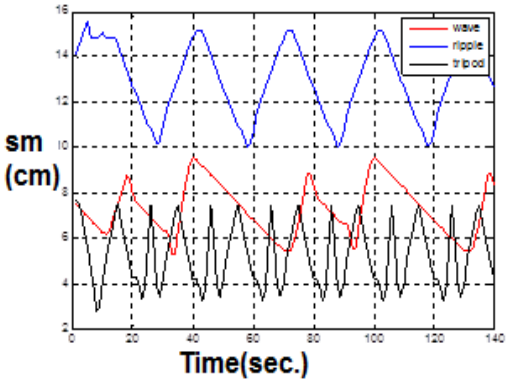

Figure 28. The stability margin for three gaits

Fig. 28 Shows that all the cases of the stability margins for a-Tripple gait (sm_1,sm_2,sm_3,sm_4), b-Wave gait (sm_1,sm_2,sm_3,sm_4,sm_5,sm_6) and c-Tripod gait(sm_1,sm_2).

6. Conclusion

In this paper the stability margins for all periodic gaits are analyzed and compared between the cases of each gait. The gaits are statically stable because the stability margins are positive values which meet the leg's constraint workspaces. In our path planning from the start point to the goal point shows clearly that the tripod gait is the fastest gait because of the less moving steps and time period. In a comparison with the wave and the ripple gaits are needed a long time and more steps. Computing the stability margins for these gaits during the path planning process shows that the ripple gait has higher stability margins than the wave gait which is also has a higher stability margins than the tripod gait.

References

[1] Xilun Ding, Zhiying Wang, Alberto Rovetta and J.M. Zhu, "Locomotion Analysis of Hexapod Robot, Climbing and Walking Robots," Behnam Miripour (Ed.), 2010.

[2] D.J. Todd, "Walking Machine: An introduction to legged robots," British Library Cataloguing in Publication Data, Anchor Press Ltd, 1985.

[3] Mohammad Imtiyaz Ahmad, Dilip Kumar Biswas and S. S Roy, "Gait Analysis of eight legged robot," International Journal of Mechanical and Industrial Engineering (IJMIE), ISSN No. 2231 –6477, Vol. 2, Issue-2, 2012.

[4] Bojan Jakimovski, "Biologically Inspired Approaches for Locomotion, Anomaly Detection and Reconfiguration for Walking Robots," Springer-Verlag Berlin Heidelberg, 2011.

[5] Shin Min Song and ByoungSoo Choi, "The Optimally Stable Ranges of 2n-Legged Wave Gaits," IEEE Trans. on system, man, and cybernetics,Vol. 20, No. 4, Jul./Aug. 1990.

[6] Mustafa SuphiErden and Kemal Leblebicioglu, "Analysis of wave gaits for energy efficiency," Springer Science+Business Media, LLC 2007.

[7] Christian Ridderstrom, "Stability of statically balanced stances for legged robots with compliance," Proceedings of the 2002 IEEE lntemational Conference on Robotics 8 Automation Washington, DC May 2002.

[8] Krzysztof W., Dominik B. and Andrzej K., "Control and environment sensing system for a six-legged robot,", Journal of Automation, Mobile Robotics & Intelligent Systems, Vol. 2, No. 3, 2008.

[9] J. Barreto, A. Trigo, P. Menezes, Dias J., "Kinematic and dynamic modeling of a six legged robot," citeseer, 2004.

[10] MĂnoiu-OlaruSorin, NiţulescuMircea, "Matlab Simulator for Gravitational Stability Analysis of a Hexapod Robot," The Romanian Review PrecisionMechanics, Optics & Mechatronics, 158 2011, No. 39 Mechanics, Optics & Mechatronics, 2011.

[11] http://www.lynxmotion.com/c-100-bh3-r.aspx, Accessed on 17/11/2013.

[12] Schilling R. J., "Fundamentals of robotics: analysis and control", ISBN: 0-13-344433-3, Prentice Hall, New Jersey, USA, 1990.

[13] R. B. McGhee and G. I. Iswandhi, "Adaptive locomotion of a multilegged robot over rough terrain," IEEE Trans. Syst., Man, Cybern., vol. SMC-9, no. 4, pp. 176–182, 1979.

[14] Stanley Kwok-Kei Chu and Grantham Kwok-Hung Pang, "Comparison between Different Model of Hexapod Robot in Fault-Tolerant Gait," IEEE Trans. Syst. Man Cybern,—PART A: Systemand Humans, VOL. 32, NO. 6, November 2002.

[15] Charles Andrew Schue, "Simulation of Tripod gaits for a Hexapod underwater walking machine," Master's Thesis, Naval Postgraduate School Monterey, California, June 1993.

[16] Sigurd Villumsen, "Modeling and Control of a six legged mobile robot," Master Thesis; 1. September 2009 - 23 of June 2010.

[17] Mohammad ali Shahriari, Kambiz Ghaemi Osguie, Amir Ali Akbar Khayyat, "Modular Framework Kinematic and Fuzzy Reward Reinforcement Learning Analysis of a Radially Symmetric Six-Legged Robot," Life Science Journal 2013.